Supporting Information

Dissecting transmembrane bicarbonate transport by 1,8-di(thio)amidocarbazoles

Krystyna Maslowska-Jarzyna,[a] Alessio Cataldo,[b] Anna Marszalik,[c] Ilona Ignatikova,[c] Stephen J. Butler,[d] Radosław Stachowiak,[c] Michał J. Chmielewski*[a] and Hennie Valkenier*[b]

[a] *Faculty of Chemistry, Biological and Chemical Research Centre, University of Warsaw, Żwirki i Wigury 101, 02-089 Warsaw, Poland*

[b] *Université libre de Bruxelles, Engineering of Molecular NanoSystems, Ecole polytechnique de Bruxelles, Avenue F.D. Roosevelt 50, CP165/64, 1050 Brussels, Belgium*

[c] *Department of Bacterial Physiology, Institute of Microbiology, Faculty of Biology, University of Warsaw, Miecznikowa 1, 02-096 Warsaw, Poland*

[d] *Loughborough University, Department of Chemistry, Epinal Way, LE11 3TU, Loughborough, United Kingdom*

E-mail: mchmielewski@chem.uw.edu.pl

E-mail: hennie.valkenier@ulb.be

Contents

1 General Information

1.1 Abbreviations and acronyms

CCCP: carbonyl cyanide *m*-chlorophenyl hydrazone;

DMSO: dimethyl sulfoxide;

HEPES: 4-(2-hydroxyethyl)-1-piperazine-ethanesulfonic acid;

HPTS: 8-hydroxypyrene-1,3,6-trisulfonic acid;

Gluc: gluconate;

LUV: large unilamellar vesicle;

Mon: monensin;

NMDG: *N*-methyl-D-glucamine;

POPC: 1-palmitoyl-2-oleoylphosphatidylcholine;

TBAOH: tetrabutylammonium hydroxide;

LB: lysogeny broth;

MIC: minimum inhibitory concentration;

IC_{50}: half maximal inhibitory concentration;

Vln: valinomycin.

1.2 Instruments and Methods

Fluorescence spectroscopy

Fluorescence spectra were acquired using Fluoromax-4 spectrometer equipped with temperature controller and injection port or an Agilent Cary Eclipse Fluorescence spectrophotometer equipped with a temperature controller.

Extrusion

AVESTIN LiposoFast-Basic extruder with polycarbonate membranes with pore sizes of 200 nm was used for extrusion during LUVs preparation.

Optical density measurements

Optical density measurements were carried out with SpectraMax iD3 Molecular Devices Multi-Mode Microplate Reader.

1.3 Materials

Transporters **1**-**4** were obtained as described previously.[1]

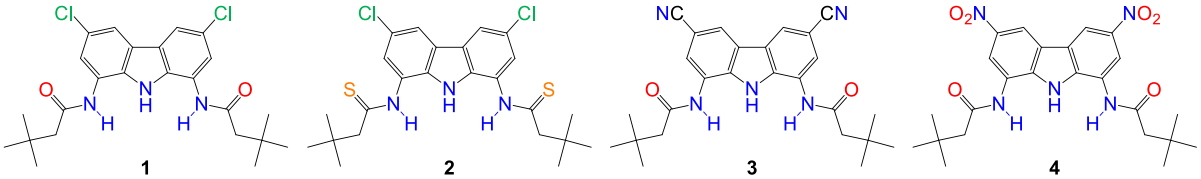

All solvents and reagents were commercially available and used as received unless otherwise stated. Water was taken from Milli-Q purification system.

[1] Amide **1**: K. M. Bąk, K. Chabuda, H. Montes, R. Quesada, M. J. Chmielewski, 1,8-Diamidocarbazoles: An Easily Tuneable Family of Fluorescent Anion Sensors and Transporters. *Org. Biomol. Chem.* **2018**, *16*, 5188–5196.
Thioamide **2**: K. M. Bąk, B. van Kolck, K. Maslowska-Jarzyna, P. Papadopoulou, A. Kros, M. J. Chmielewski, Oxyanion Transport across Lipid Bilayers: Direct Measurements in Large and Giant Unilamellar Vesicles. *Chem. Commun.* **2020**, *56*, 4910–4913.
Amides **3**-**4**: K. Maslowska-Jarzyna, M. L. Korczak, J. A. Wagner, M. J. Chmielewski, Carbazole-Based Colorimetric Anion Sensors. *Molecules* **2021**, *26*, 3205–3221.

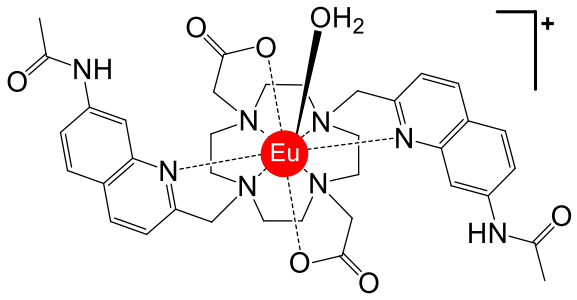

[Eu.L^1]$^+$

Eu(III) complex [Eu.L^1]$^+$ was synthesised according to the protocol described previously[2] and purified by preparative reverse-phase HPLC [gradient: 2-100% acetonitrile in 25 mM NH_4CO_3 over 15 min; t_R = 6.75 min], to give [Eu.L^1]$^+$ as a colourless solid (7 mg, 65%).

^{1}H NMR (400 MHz, D_2O) spectral range of 77 ppm (+47.2 to -30.0 ppm), 47.3, 29.6, 17.8, 16.4, 16.0, 15.2, 14.7, 13.1, 11.8, 11.0, 9.4, 9.1, 7.0, 6.0, 4.0, 3.4, 2.8, 2.4, 1.9, 1.7, -0.5, -2.1, -2.2, -5.6, -6.5, -7.3, -12.0, -12.4, -14.0, -17.4, -18.7, -27.8, -28.1, -30.0, two signals obscured or overlapping, N-H signals not observed; ESI-HRMS(+) *m/z* 833.2444 [M(^{151}Eu)]$^+$ ($C_{36}H_{42}N_8O_6{}^{151}Eu$ requires 833.2426); τ_{H2O} = 0.48 ms; τ_{D2O} = 1.39 ms; hydration state q = 1, Φ^{em}_{H2O} = 7% (± 15%); ε_{H2O} (332 nm) = 12,500 M^{-1} cm^{-1}.

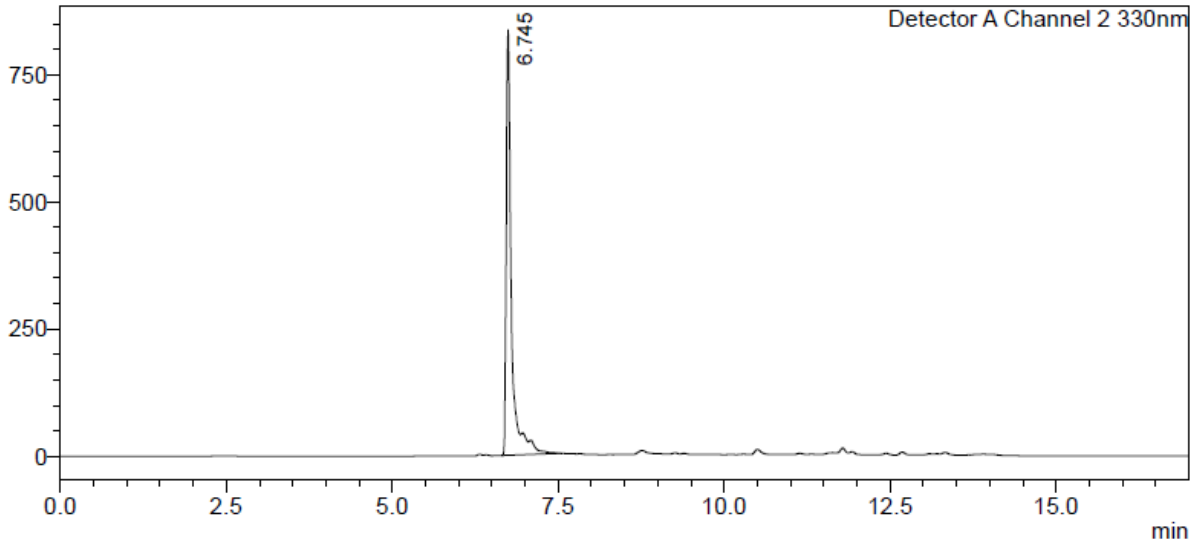

Analytical RP-HPLC trace of [Eu.L^1]$^+$ showing t_R = 6.75 min [gradient: 2-100% acetonitrile in 25 mM NH_4CO_3 over 15 minutes].

[2] S. J. Butler, Quantitative determination of fluoride in pure water using luminescent europium complexes. *Chem. Commun.*, **2015**, *51*, 10879–10882.

2 Bicarbonate transport studies using EuL1 assay

2.1 General procedure for bicarbonate transport studies using EuL1 assay

To study bicarbonate transport, direct EuL1 assay was used that was developed previously.[3] LUVs made of POPC and cholesterol in a 7:3 molar ratio were prepared as follows. In a 5 mL round bottom flask, a solution of lipids (POPC and cholesterol in a 7:3 molar ratio) in chloroform (freshly deacidified by passing through a pad of activated basic alumina) was prepared.

The chloroform was evaporated under a flow of nitrogen and the thus-prepared lipid film was further dried under vacuum for at least 1 h. The lipid film was hydrated with 500 μL of a buffered aqueous solution containing $[Eu.L^1]^+$ probe (50 μM, prepared from a 5 mM stock solution in methanol), NaCl (225 mM) and HEPES (5 mM, pH 7), sonicated for 30 s and stirred for 1 h to give heterogeneous vesicles. The suspension was subjected to 10 freeze/thaw cycles, diluted to 1 mL by the addition of 500 μL of buffer solution and extruded 29 times through a 200 nm polycarbonate membrane. The unentrapped $[Eu.L^1]^+$ was removed by size exclusion chromatography on a Sephadex G25 column using the NaCl/HEPES buffer solution as eluent. The collected vesicles were diluted with the eluent to obtain total lipid concentration of ≈ 0.4 mM.

The liposome suspension (3.00 mL) was placed in a quartz cuvette equipped with a small stirring bar and the temperature was allowed to stabilize at 25 °C for 3-5 min. inside the sample compartment of a Fluoromax-4 spectrometer. The spectrometer was equipped with a 495 nm cut-off filter between the sample and the detector. DMSO alone (5 μL, blank) or DMSO solution of transporters **1**-**4** (16.7 μL of 2.4 mM or 5 μL of 2.4 mM, 0.8 mM, 0.24 mM 0.08 mM, 24 μM, 8 μM, 2.4 μM, 0.8 μM, 0.24 μM to achieve 1:30, 1:100, 1:300, 1:1k, 1:3k, 1:10k, 1:30k, 1:100k, 1:300k or 1:1m transporter:lipids ratio, respectively) was added to the vesicle suspension and the temperature was equilibrated at 25°C for 2 min prior to the addition of bicarbonate. If the cation transporter monensin was used, it was added to the liposomes as a solution in methanol (5 μL of 0.24 mM solution, to create a 1:1k cation transporter:lipids ratio).

The emission or the $[Eu.L^1]^+$ probe (λ_{ex}= 330 nm, λ_{em}= 615 nm) was recorded as a function of time over 15 min. An aqueous solution of $NaHCO_3$ (38 μL, 0.8 M in 225 mM NaCl and 5 mM HEPES) was added to the vesicle suspension 30 s after the start of the emission recording, to create bicarbonate concentration gradient of 10 mM. Detergent (Triton X-100, 50 μL, 5% w/w in water) was added 10 minutes after the addition of bicarbonate to lyse the liposomes. Emission data were collected for three runs. The data were normalised from 0 (before the addition of HCO_3^-) to 1 (after lysis).

[3] L. Martínez-Crespo, S. H. Hewitt, N. A. de Simone, V. Šindelář, A. P. Davis, S. Butler, H. Valkenier, Transmembrane Transport of Bicarbonate Unravelled. *Chem. Eur. J.*, **2021**, *27*, 7367–7375.

2.2 Bicarbonate transport in buffered NaCl at different concentrations of **1**-**4**

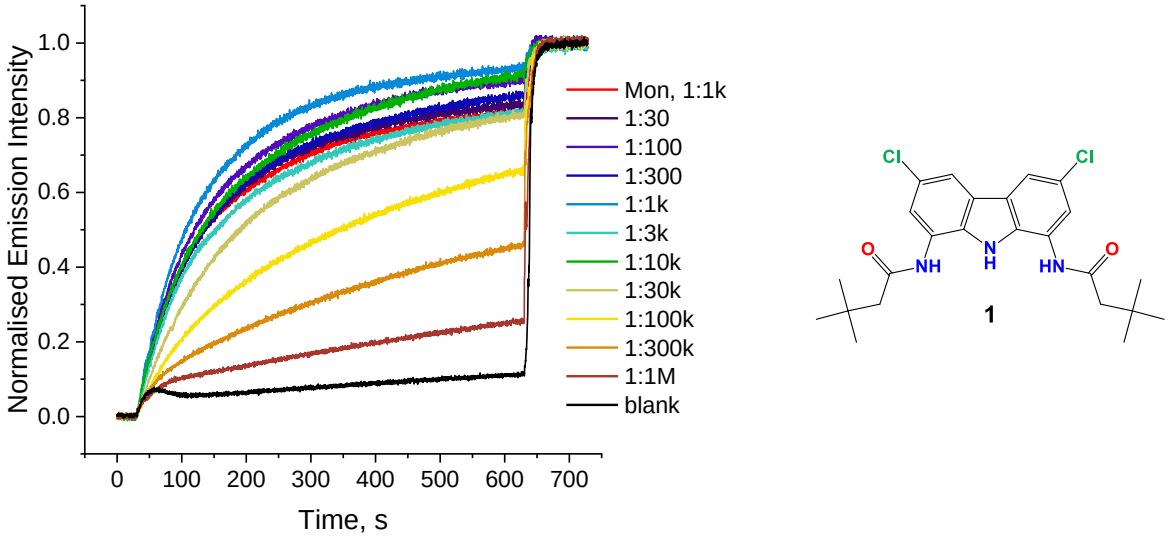

Figure S2.2.1. Normalised emission intensity as a function of time in bicarbonate transport by **1** at various transporter:lipids ratios, monitored by means of the EuL1 assay. Buffer composition: 225 mM NaCl + 5 mM HEPES, pH 7. 10 mM sodium bicarbonate was added at t = 30 s. The LUVs were lysed after 10 minutes of acquisition. Transporter was added as a solution in DMSO.Transporter was added as DMSO solutions.

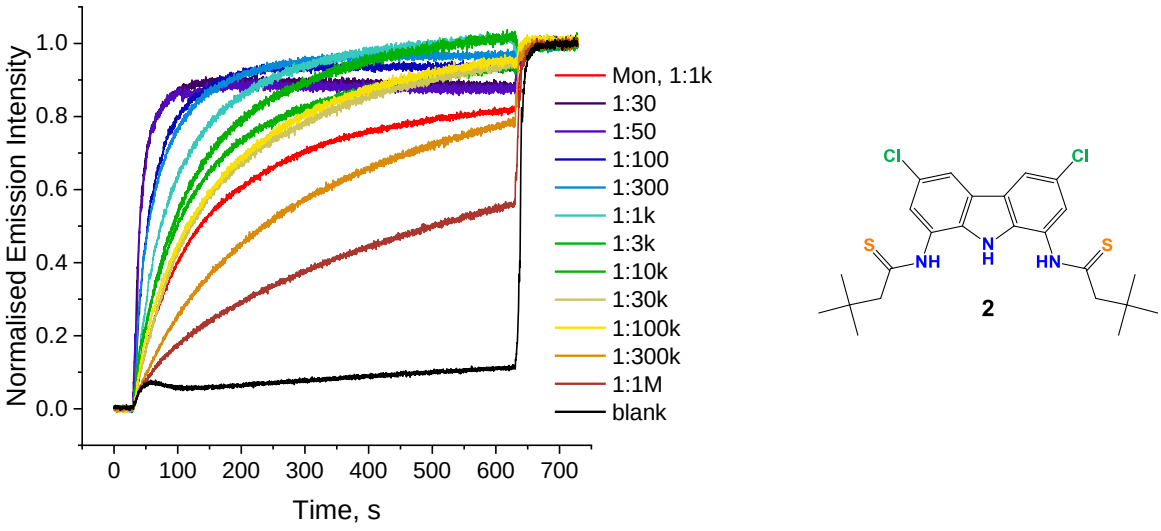

Figure S2.2.2. Normalised emission intensity as a function of time in bicarbonate transport by **2** at various transporter:lipids ratios, monitored by means of the EuL1 assay. Buffer composiotion: 225 mM NaCl + 5 mM HEPES, pH 7. 10 mM sodium bicarbonate was added at t = 30 s. The LUVs were lysed after 10 minutes of acquisition. Transporter was added as a solution in DMSO.

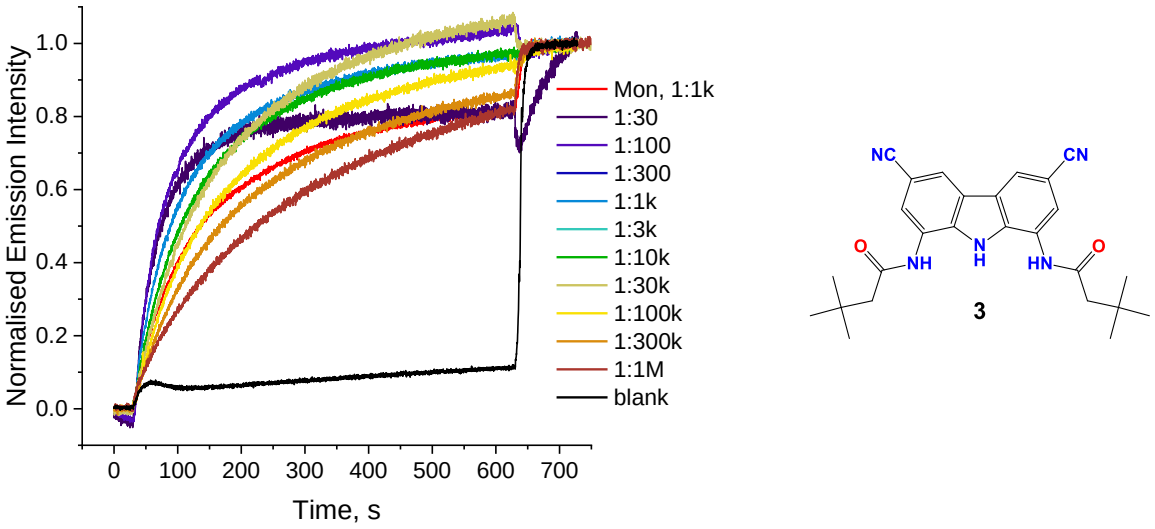

Figure S2.2.3. Normalised emission intensity as a function of time in bicarbonate transport by **3** at various transporter:lipids ratios, monitored by means of the EuL1 assay. Buffer composiotion: 225 mM NaCl + 5 mM HEPES, pH 7. 10 mM sodium bicarbonate was added at t = 30 s. The LUVs were lysed after 10 minutes of acquisition. Transporter was added as a solution in DMSO.

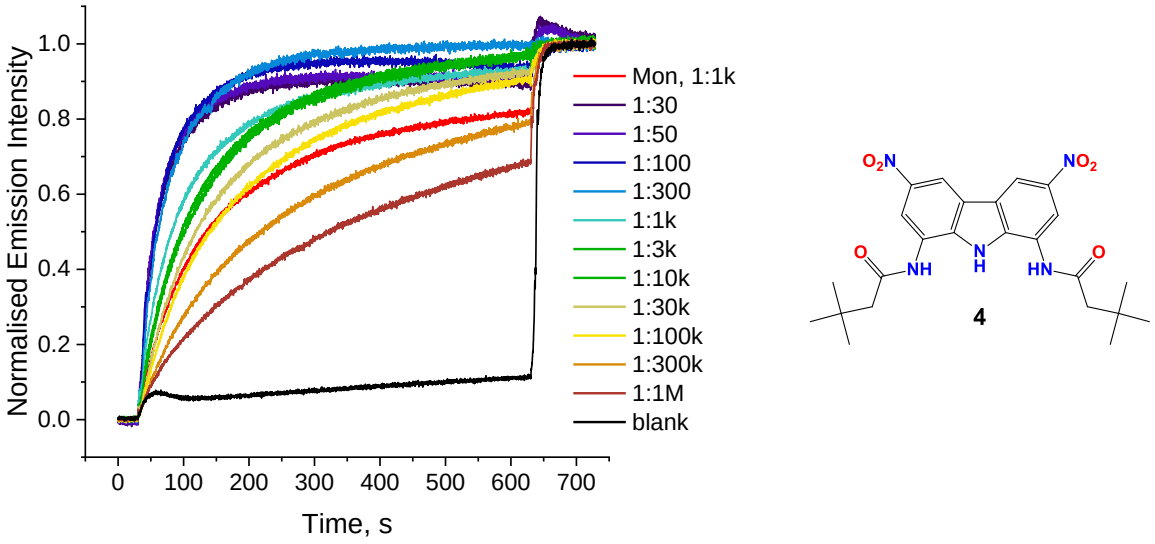

Figure S2.2.4. Normalised emission intensity as a function of time in bicarbonate transport by **4** at various transporter:lipids ratios, monitored by means of the EuL1 assay. Buffer composiotion: 225 mM NaCl + 5 mM HEPES, pH 7. 10 mM sodium bicarbonate was added at t = 30 s. The LUVs were lysed after 10 minutes of acquisition. Transporter was added as a solution in DMSO.

2.3 Quantification of the transport rates

Data fitting to obtain transport rates was performed using Origin 2022. The first 30 seconds of averaged and normalised data were removed, leaving addition of $NaHCO_3$ at t = 0 s and next 550 s of the traces were fitted with a single exponential decay function:

$$F = y - a \cdot \exp(-k \cdot t),$$

where y, a and k were treated as fitting parameters.

2.4 Determination of bicarbonate transport rates at different concentrations of **1**

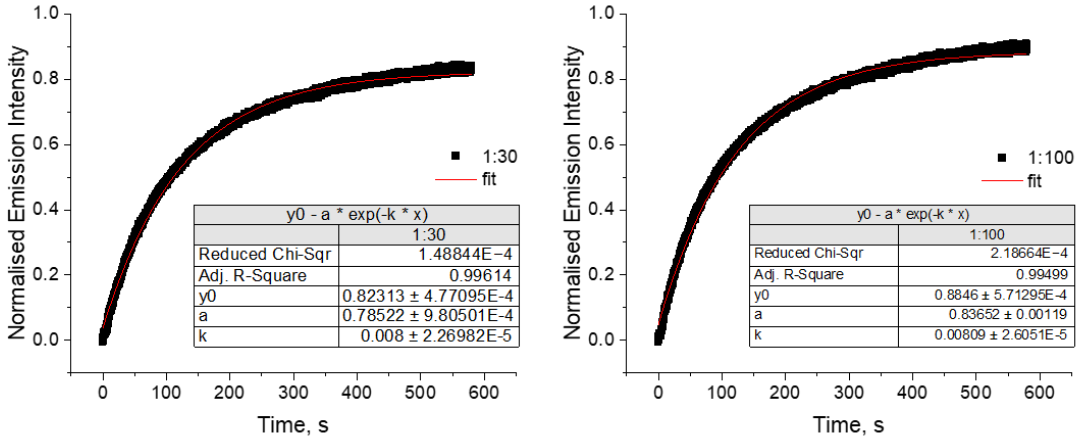

Figure S2.4.1. Normalised emission intensity and single exponential fit for the transport of HCO_3^- with transporter **1** at 1:30 (left) and 1:100 (right) transporter:lipids ratio.

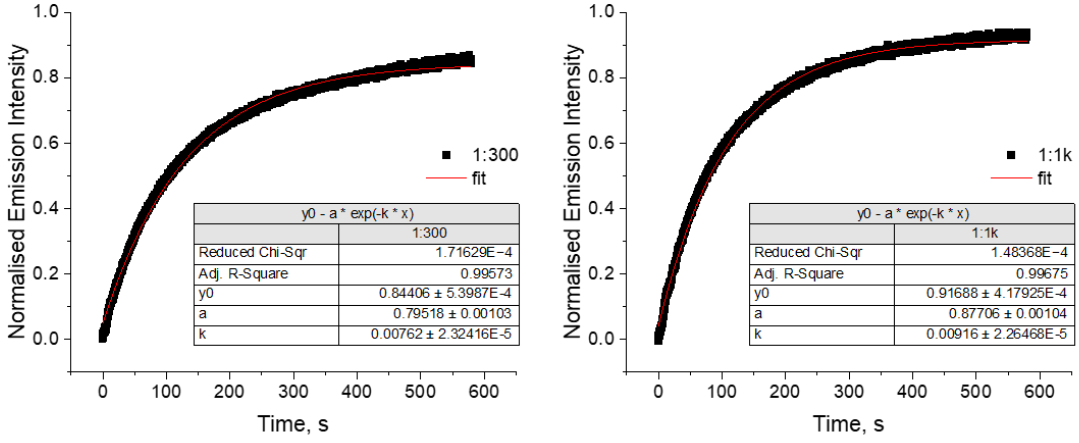

Figure S2.4.2. Normalised emission intensity and single exponential fit for the transport of HCO_3^- with transporter **1** at 1:300 (left) and 1:1k (right) transporter:lipids ratio.

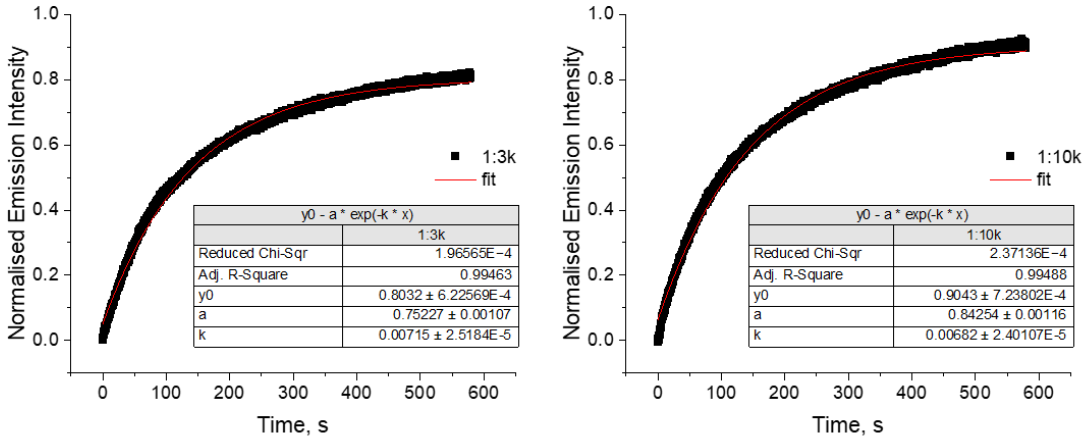

Figure S2.4.3. Normalised emission intensity and single exponential fit for the transport of HCO_3^- with transporter **1** at 1:3k (left) and 1:10k (right) transporter:lipids ratio.

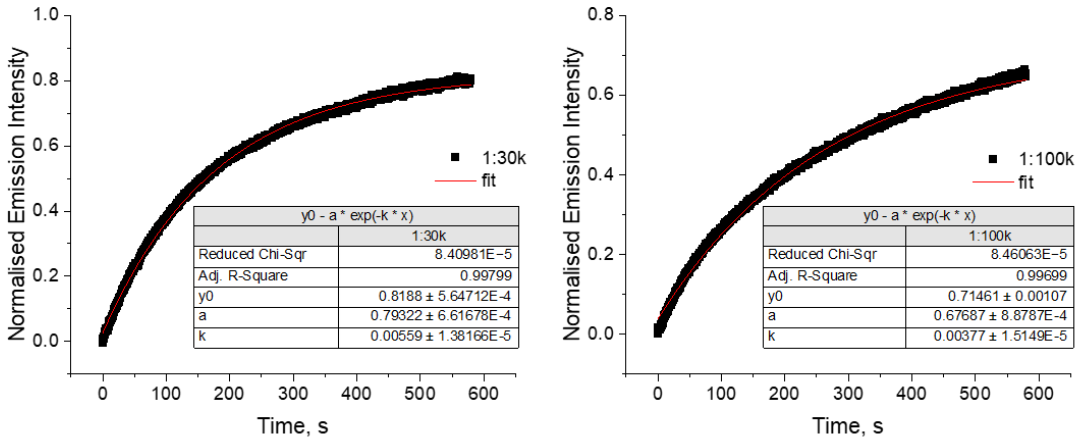

Figure S2.4.4. Normalised emission intensity and single exponential fit for the transport of HCO_3^- with transporter **1** at 1:30k (left) and 1:100k (right) transporter:lipids ratio.

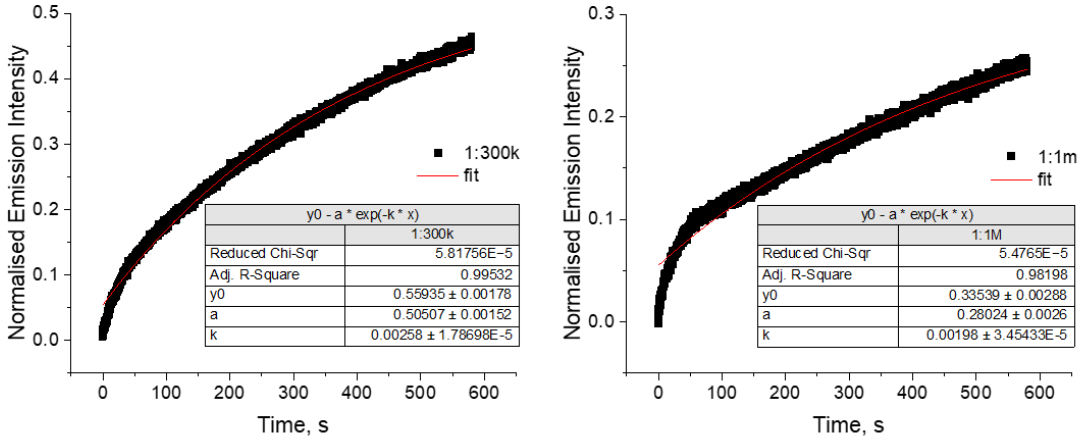

Figure S2.4.5. Normalised emission intensity and single exponential fit for the transport of HCO_3^- with transporter **1** at 1:300k (left) and 1:1m (right) transporter:lipids ratio.

2.5 Determination of bicarbonate transport rates at different concentrations of **2**

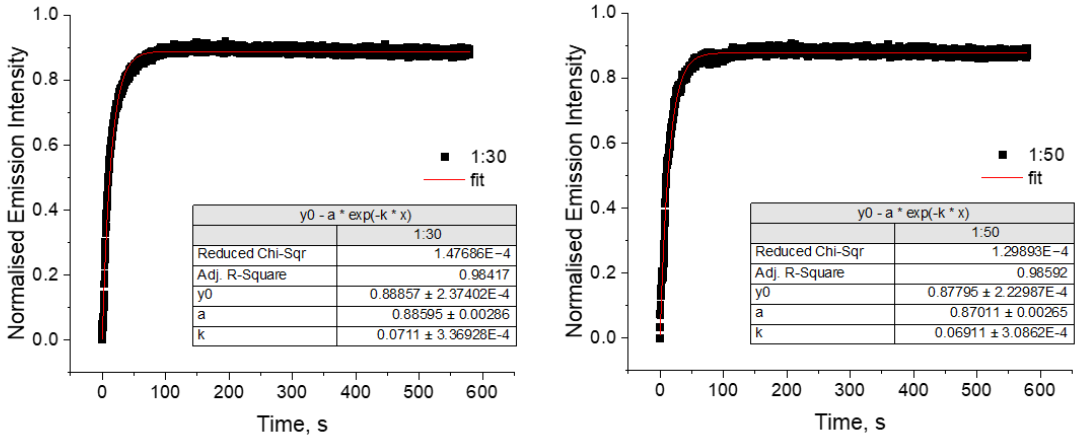

Figure S2.5.1. Normalised emission intensity and single exponential fit for the transport of HCO_3^- with transporter **2** at 1:30 (left) and 1:50 (right) transporter:lipids ratio.

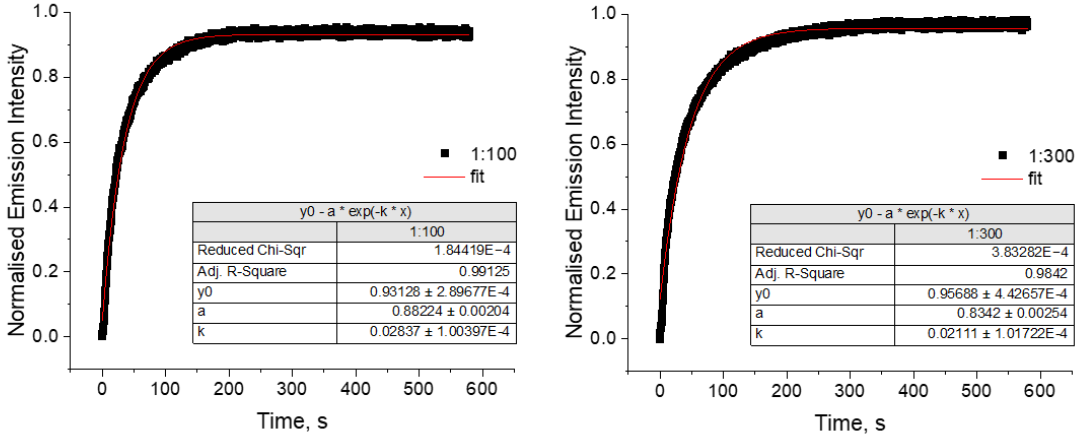

Figure S2.5.2. Normalised emission intensity and single exponential fit for the transport of HCO_3^- with transporter **2** at 1:100 (left) and 1:300 (right) transporter:lipids ratio.

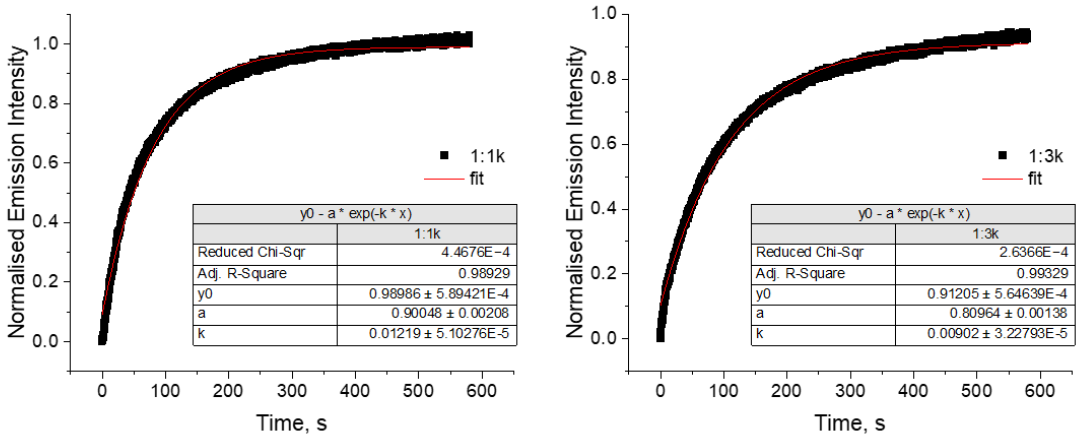

Figure S2.5.3. Normalised emission intensity and single exponential fit for the transport of HCO_3^- with transporter **2** at 1:1k (left) and 1:3k (right) transporter:lipids ratio.

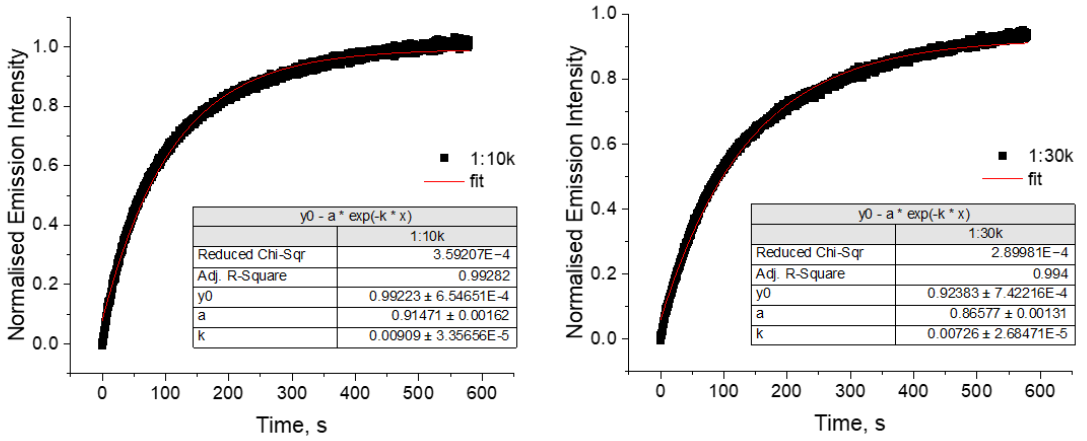

Figure S2.5.4. Normalised emission intensity and single exponential fit for the transport of HCO_3^- with transporter **2** at 1:10k (left) and 1:30k (right) transporter:lipids ratio.

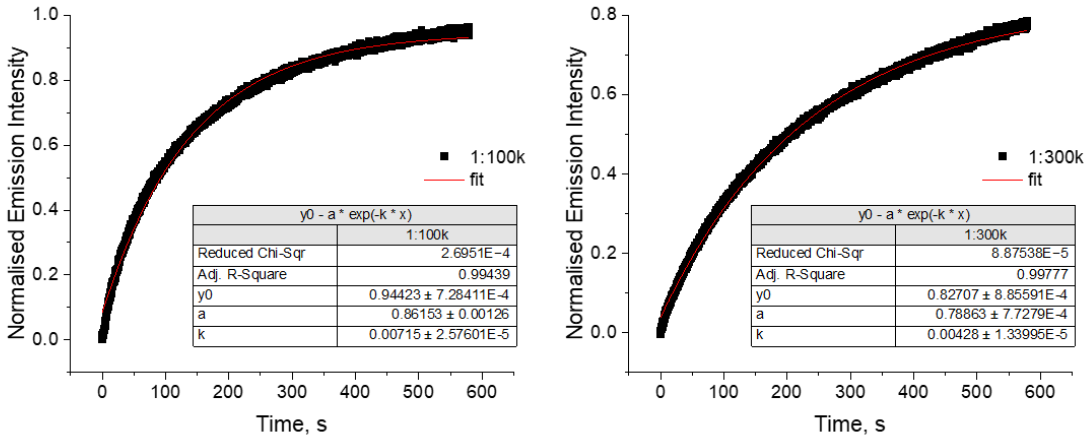

Figure S2.5.5. Normalised emission intensity and single exponential fit for the transport of HCO_3^- with transporter **2** at 1:100k (left) and 1:300k (right) transporter:lipids ratio.

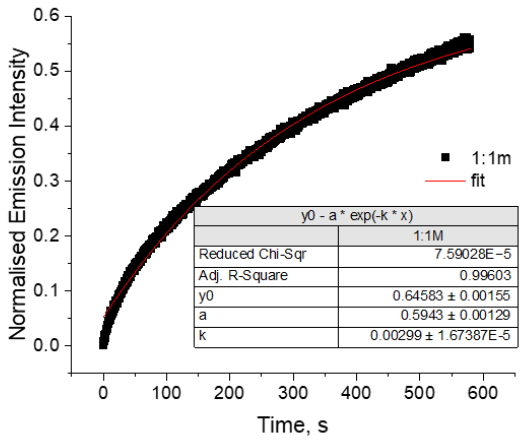

Figure S2.5.6. Normalised emission intensity and single exponential fit for the transport of HCO_3^- with transporter **2** at 1:1m transporter:lipids ratio.

2.6 Determination of bicarbonate transport rates at different concentrations of **3**

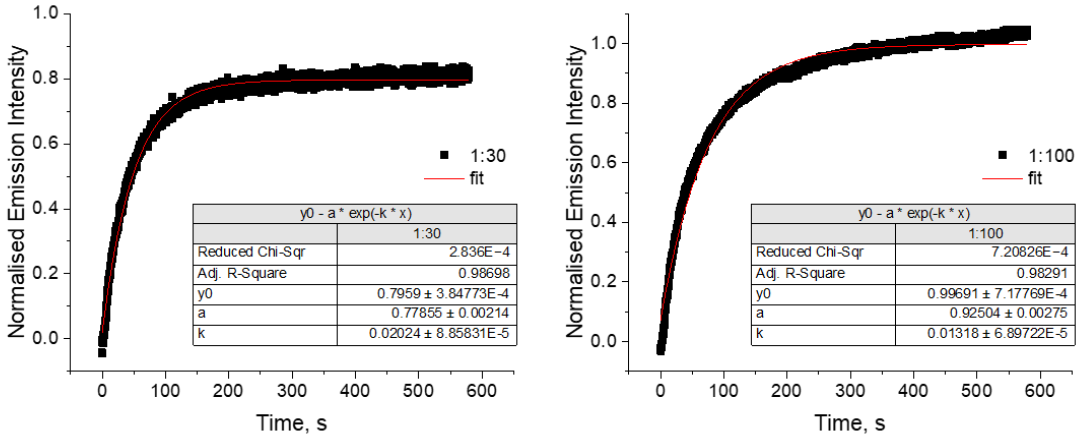

Figure S2.6.1. Normalised emission intensity and single exponential fit for the transport of HCO_3^- with transporter **3** at 1:30 (left) and 1:100 (right) transporter:lipids ratio.

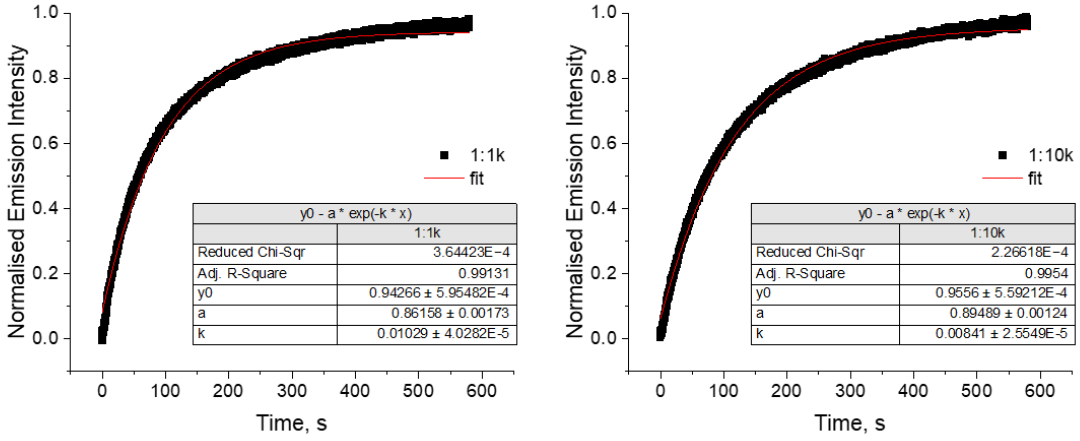

Figure S2.6.2. Normalised emission intensity and single exponential fit for the transport of HCO_3^- with transporter **3** at 1:1k (left) and 1:10k (right) transporter:lipids ratio.

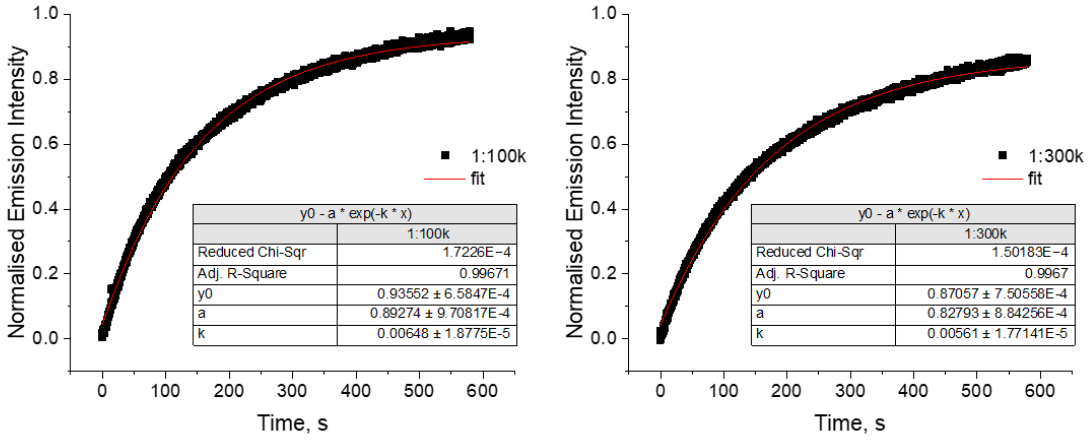

Figure S2.6.3. Normalised emission intensity and single exponential fit for the transport of HCO_3^- with transporter **3** at 1:100k (left) and 1:300k (right) transporter:lipids ratio.

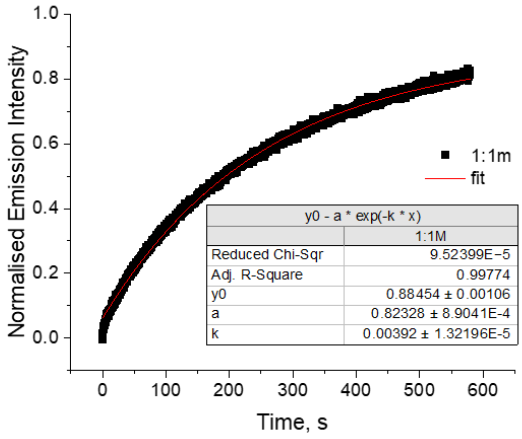

Figure S2.6.4. Normalised emission intensity and single exponential fit for the transport of HCO_3^- with transporter **3** at 1:1m transporter:lipids ratio.

2.7 Determination of bicarbonate transport rates at different concentrations of **4**

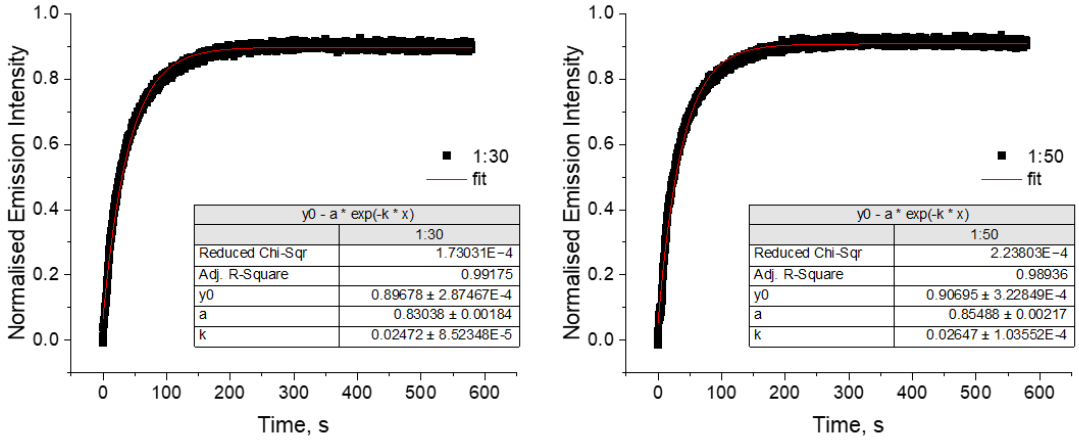

Figure S2.7.1. Normalised emission intensity and single exponential fit for the transport of HCO_3^- with transporter **4** at 1:30 (left) and 1:50 (right) transporter:lipids ratio.

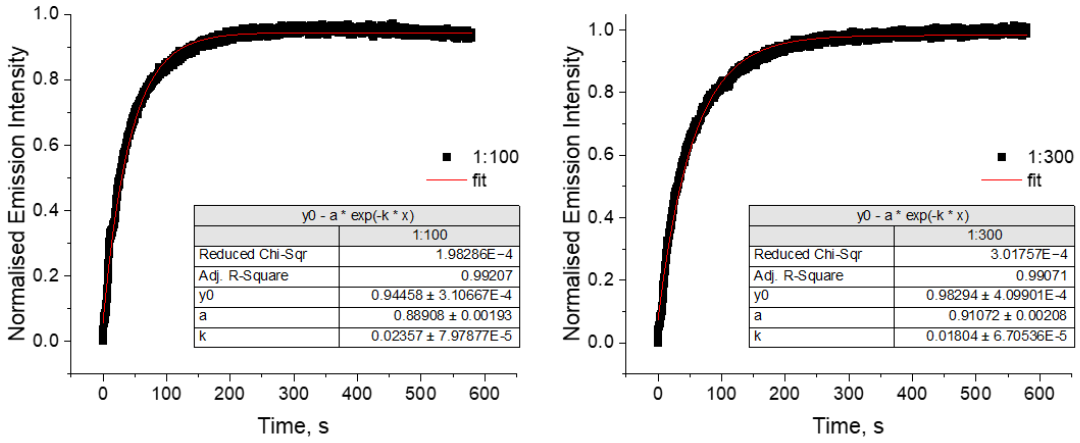

Figure S2.7.2. Normalised emission intensity and single exponential fit for the transport of HCO_3^- with transporter **4** at 1:100 (left) and 1:300 (right) transporter:lipids ratio.

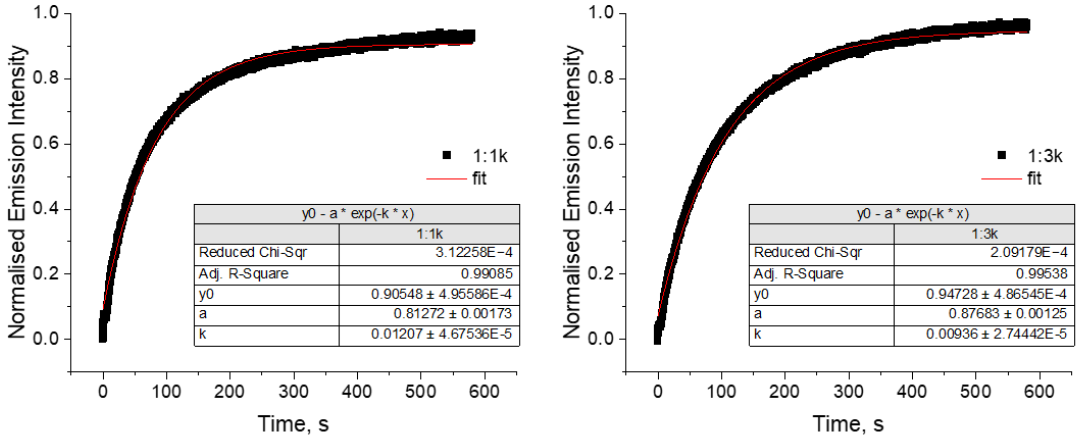

Figure S2.7.3. Normalised emission intensity and single exponential fit for the transport of HCO_3^- with transporter **4** at 1:1k (left) and 1:3k (right) transporter:lipids ratio.

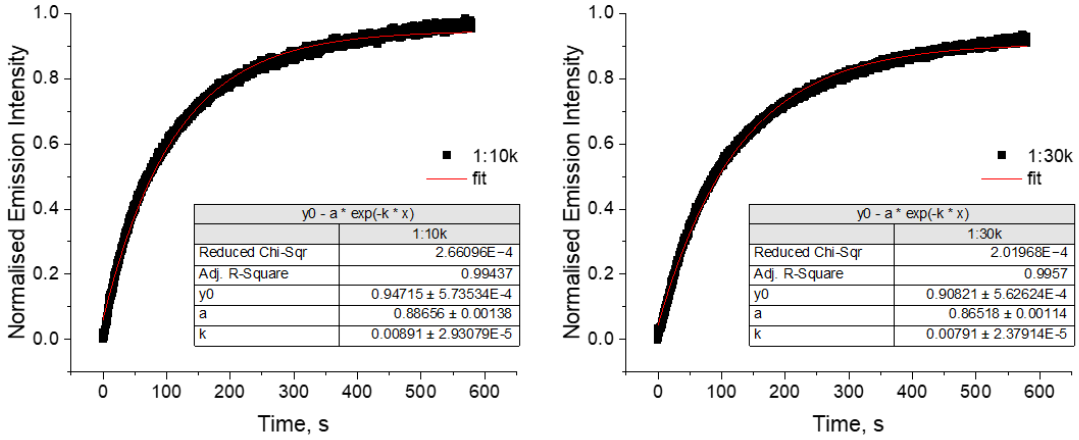

Figure S2.7.4. Normalised emission intensity and single exponential fit for the transport of HCO_3^- with transporter **4** at 1:10k (left) and 1:30k (right) transporter:lipids ratio.

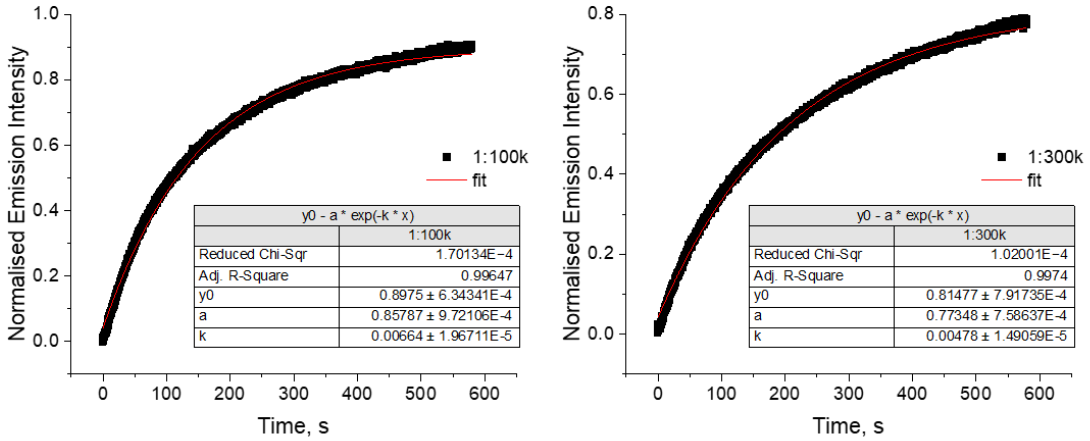

Figure S2.7.5. Normalised emission intensity and single exponential fit for the transport of HCO_3^- with transporter **4** at 1:100k (left) and 1:300k (right) transporter:lipids ratio.

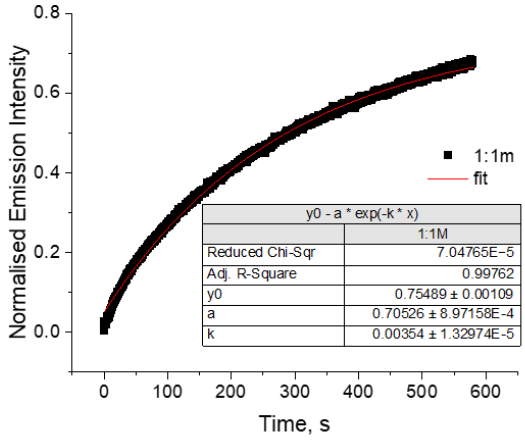

Figure S2.7.6. Normalised emission intensity and single exponential fit for the transport of HCO_3^- with transporter **4** at 1:1m transporter:lipids ratio.

2.8 Determination of transport rate of CO_2 diffusion

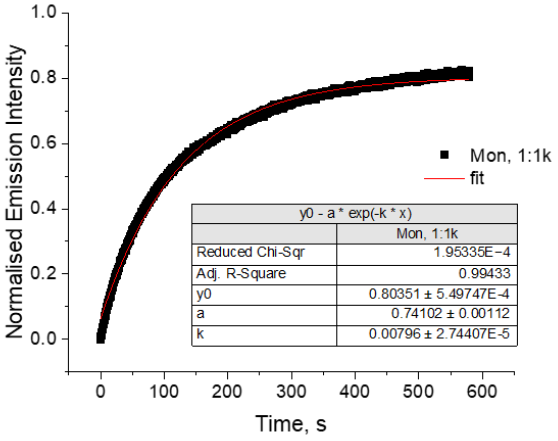

Figure S2.8.1. Normalised emission intensity and single exponential fit for the CO_2 diffusion assisted by pH and charge gradients dissipation by monensin at 1:1k transporter:lipids ratio.

2.9 Bicarbonate transport by **1**-**4** in buffered NaCl, in the absence and presence of monensin

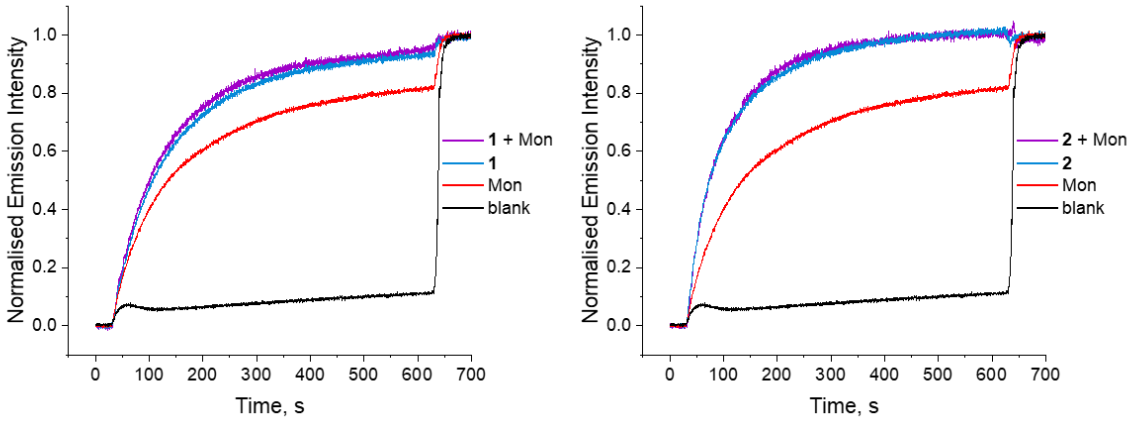

Figure S2.9.1. Normalised emission intensity as a function of time in bicarbonate transport by **1** and **1**+Mon (left) or **2** and **2**+Mon (right), monitored by the EuL1 assay in 225 mM NaCl with 5 mM HEPES at pH 7, upon addition of 10 mM $NaHCO_3$. Sodium bicarbonate was added at t = 30 s. Transporters **1**, **2** and monensin were added to the LUVs at 1:1k transporter to lipids ratio. The LUVs were lysed after 10 minutes of acquisition.

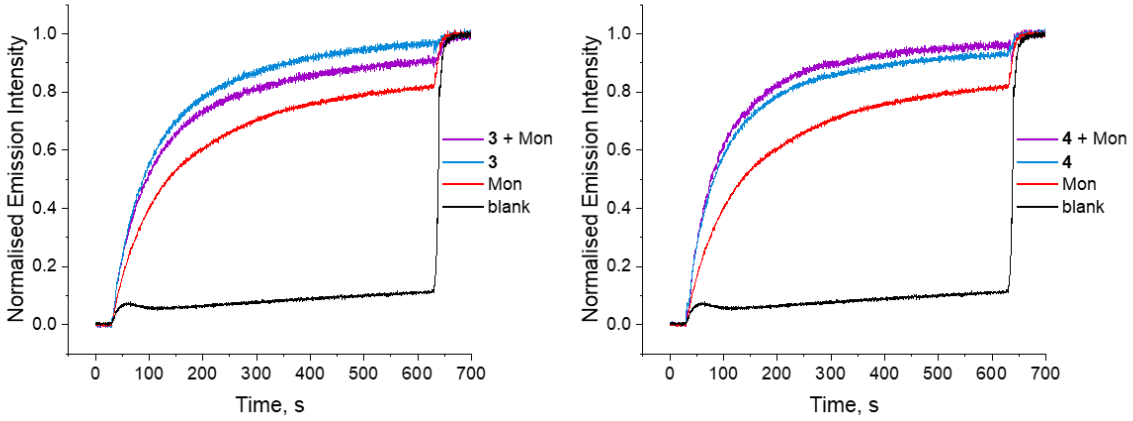

Figure S2.9.2. Normalised emission intensity as a function of time in bicarbonate transport by **3** and **3**+Mon (left) or **4** and **4**+Mon (right), monitored by the EuL1 assay in 225 mM NaCl with 5 mM HEPES at pH 7, upon addition of 10 mM $NaHCO_3$. Sodium bicarbonate was added at t = 30 s. Transporters **3**, **4** and monensin were added to the LUVs at 1:1k transporter to lipids ratio. The LUVs were lysed after 10 minutes of acquisition.

Data fitting to obtain transport rates was performed according to the procedure described in Section 2.3. The comparison of the transport rate constants with and without monensin is shown in the Table below:

	1	**2**	**3**	**4**
$k_{\text{transporter}}$, s^{-1}	0.00926	0.01238	0.01047	0.01226
$k_{\text{transporter + monensin}}$, s^{-1}	0.00984	0.01341	0.01057	0.01307

2.10 Uniport of bicarbonate by anionophores in potassium gluconate solution

The EuL1 assay was adapted to study the uniport of HCO_3^- by replacing the NaCl by 100 mM potassium gluconate (KGluc) and by the addition of the cationophore valinomycin. A bicarbonate gradient was created by the addition of 10 mM $KHCO_3$. Gluconate anions are too hydrophilic to participate in an antiport mechanism, and therefore only the transport of K^+ by valinomycin can balance the uniport of HCO_3^- by anionophore. Indeed, we did notice an increase in fluorescence when transporter **2** or **4** was combined with valinomycin (Fig. S2.9). However, such a response in the EuL1 assay can results from two independent mechanisms:

1) true HCO_3^- uniport by anionophore accompanied by charge equilibration via K^+ transport by Vln
   or
2) CO_2 diffusion across lipid bilayer, followed by pH equilibration via H^+ or OH^- uniport by an anionophore and charge equilibration via K^+ transport by Vln, which is more probable according to previous considerations.

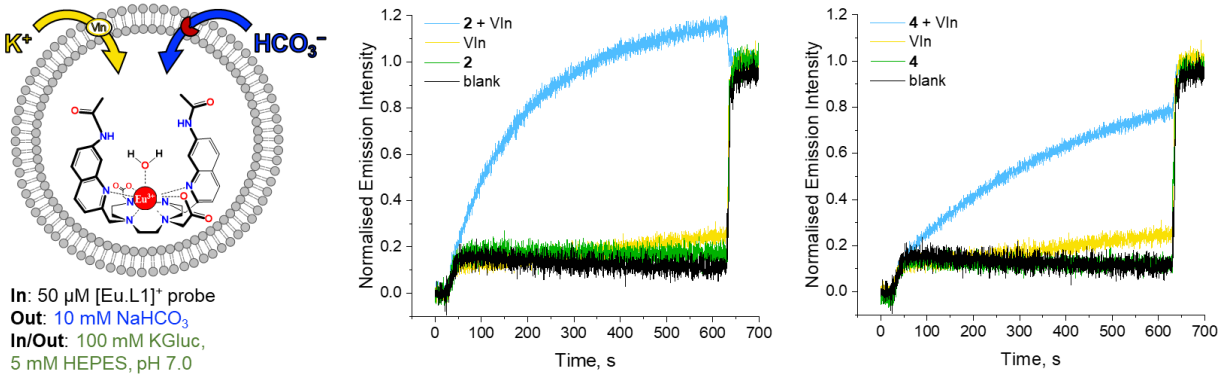

Figure S2.10. Schematic representation of the EuL1 assay for studying the uniport of HCO_3^- (left). Bicarbonate transport by anionophore **2** (1:10k, middle) or **4** (1:10k, right), valinomycin (1:1k) and the combination of **2**/**4** (1:10k) and Val (1:1k), as monitored by the EuL1 assay in 100 mM KGluc with 5 mM HEPES, pH 7, upon addition of 10 mM $KHCO_3$ at t = 30 s. The LUVs were lysed 10 minutes after the addition of $KHCO_3$.

3 Uncommon relationship between transport rate and anionophore concentration

In theory, the transport rate k of bicarbonate transport should linearly depend on the concentration of transporter in the membrane (see discussion in the main text). In the case of compounds **1**-**4**, significant deviations from linearity were observed, suggesting that more than one transport mechanism is operational (Figures S3.1-S3.4).

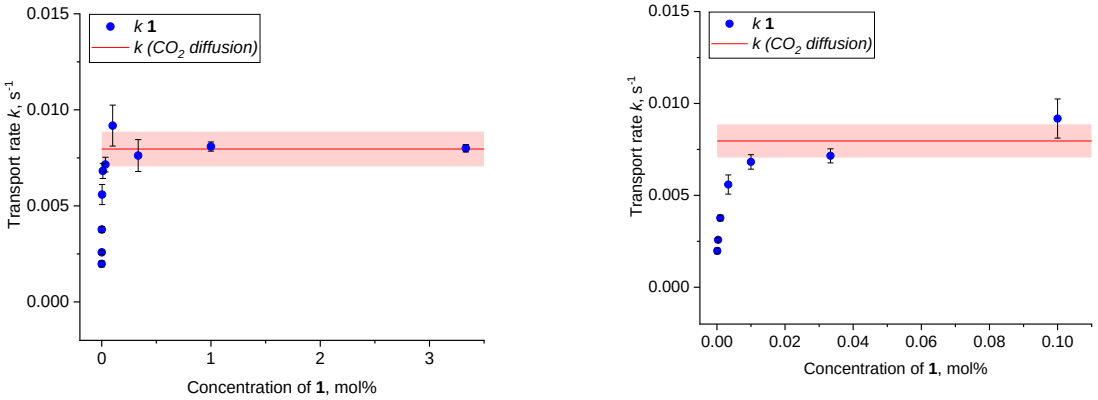

Figure S3.1. Left: plot of the transport rate k vs. concentration of **1** in mol%. The anionophore was added externally as a solution in DMSO. Right: zoom at lower concentrations of **1**.

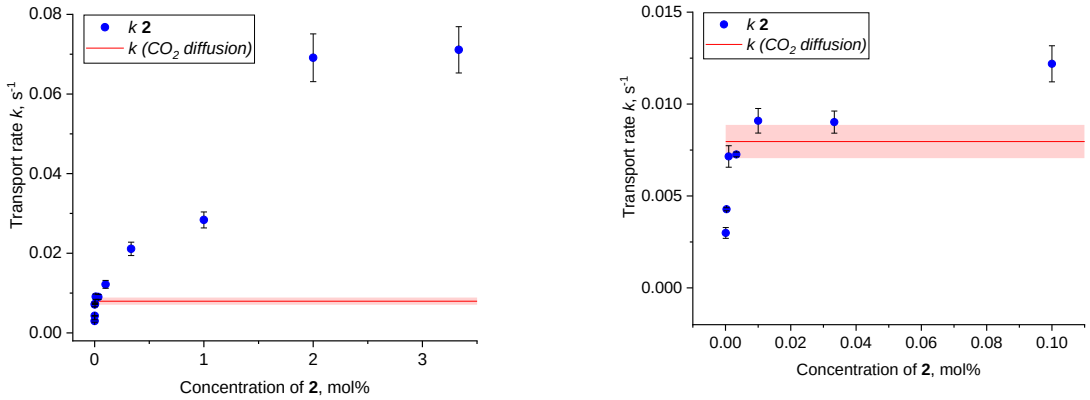

Figure S3.2. Left: plot of transport rate k vs. concentration of **2** in mol%. The anionophore was added externally as a solution in DMSO. Right: zoom at lower concentrations of **2**.

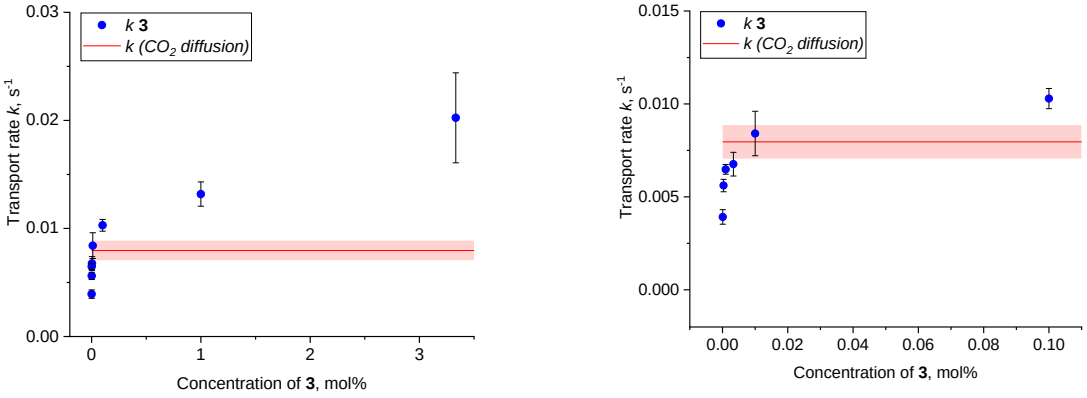

Figure S3.3. Left: plot of transport rate *k* vs. concentration of **3** in mol%. The anionophore was added externally as a solution in DMSO. Right: zoom at lower concentrations of **3**.

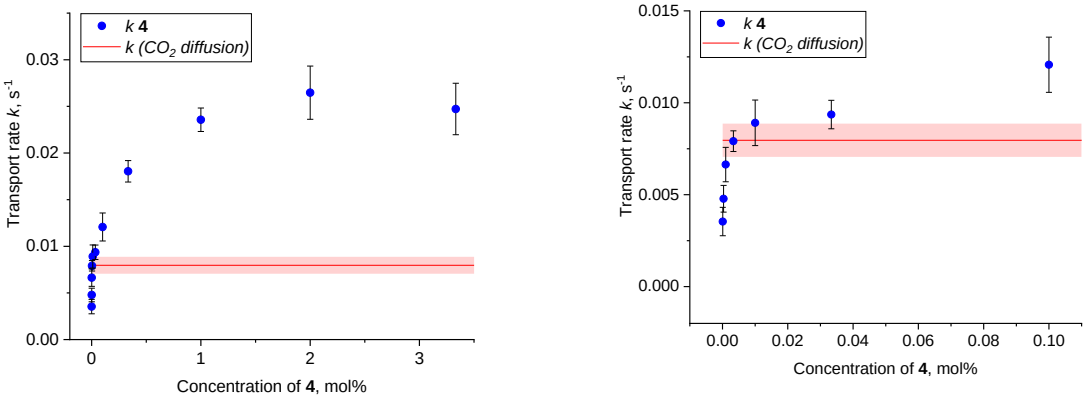

Figure S3.4. Left: plot of transport rate *k* vs. concentration of **4** in mol%. The anionophore was added externally as a solution in DMSO. Right: zoom at lower concentrations of **4**.

This peculiar concentration dependence can be explained by the co-existence of two mechanisms:

1) transmembrane CO_2 diffusion followed by hydration and pH equilibration by **1**-**4**;
2) HCO_3^- transport by the most active anionophores, via HCO_3^-/Cl^- antiport.

If both processes are independent and both follow exponential kinetics, the experimental transport rate should be the sum of their respective rate constants:

$$k_{experimental} = k_{CO_2\ diffusion} + k_{HCO_3^-\ transport}$$

The rate constant of transmembrane CO_2 diffusion can be estimated from an independent experiment with monensin as k = 0.00796. The rate of transporter-dependent bicarbonate transport can be calculated as:

$$k_{HCO_3^-\ transport} = k_{experimental} - k_{CO_2\ diffusion} = k_{experimental} - 0.0080$$

This gives us the following values of true $k_{HCO_3^-\ transport}$:

C, mol%	$k_{HCO3-\ transport}$ by:							
	1, s^{-1}	**1**, % [a]	**2**, s^{-1}	**2**, % [a]	**3**, s^{-1}	**3**, % [a]	**4**, s^{-1}	**4**, % [a]
0.0001	- [b]	- [b]	- [b]	- [b]	- [b]	- [b]	- [b]	- [b]
0.0003	- [b]	- [b]	- [b]	- [b]	- [b]	- [b]	- [b]	- [b]
0.0010	- [b]	- [b]	- [b]	- [b]	- [b]	- [b]	- [b]	- [b]
0.0033	- [b]	- [b]	-	-	-	-	- [b]	- [b]
0.0100	- [b]	- [b]	0.0011	12	0.00041	5	0.00090	10
0.0333	- [b]	- [b]	0.0010	11	-	-	0.0014	15
0.1000	0.0012	13	0.0042	34	0.0023	22	0.0041	34
0.3333	- [b]	- [b]	0.013	**62**	-	-	0.010	**56**
1.0000	0.00009	1	0.020	**72**	0.0052	39	0.016	**66**
2.0000	-	-	0.061	**88**	-	-	0.019	**70**
3.3333	-	-	0.063	**89**	0.012	**61**	0.017	**68**

[a] Relative share of the transporter-dependent bicarbonate transport (in %) = $k_{HCO_3^-\ transport} \cdot 100\%/k_{experimental}$.

[b] The difference between $k_{experimental}$ and $k_{CO_2\ diffusion}$ is less than 0, indicating no $k_{HCO_3^-\ transport}$ at this concentration.

<u>The true HCO_3^- transport dominates (**>50%**) at high concentrations of compounds **2**-**4**.</u>

4 H^+Cl^- or OH^-/Cl^- transport studies

4.1 General procedure for transport measurements using HPTS assay

LUVs made of POPC and cholesterol in a 7:3 molar ratio, were prepared as follows. In a 5 mL round bottom flask, a solution of lipids (POPC and cholesterol in a 7:3 molar ratio) in chloroform (freshly deacidified by passing through a pad of activated basic alumina) was prepared.

The solution of lipids in chloroform was evaporated under a flow of nitrogen and the thus-prepared lipid film was further dried under vacuum for at least 1 h. The lipid film was hydrated with 500 μL of a buffered aqueous solution containing HPTS (1 mM) in the desired buffer (100 mM NMDGHCl, 10 mM HEPES, pH 6.8), sonicated for 30 s and stirred for 1 h to give heterogeneous vesicles. The suspension was subjected to 10 freeze/thaw cycles, diluted to 1 mL by the addition of 500 μL of buffer solution and extruded 29 times through a 200 nm polycarbonate membrane. The unentrapped HPTS was removed by size exclusion chromatography on a Sephadex G25 column using buffer solution as eluent. The collected vesicles were diluted with the eluent to obtain total lipid concentration of ≈ 0.1 mM).

The liposome suspension (3 mL) was placed in a quartz cuvette equipped with a small stirring bar and the temperature was allowed to stabilize at 25 ˚C for 3-5 min. inside the sample compartment of an Agilent Cary Eclipse Fluorescence Spectrophotometer equipped with a stirrer plate and a temperature controller. DMSO alone (5 μL, blank) or DMSO solutions of transporters **1**-**4** (5 μL, 6 μM, 2.4 μM, 1.2 μM, 0.6 μM, 0.24 μM, 0.12 μM, 0.06 μM, 0.012 μM to achieve 1:10k, 1:25k, 1:50k, 1:100k, 1:250k, 1:500k, 1:1m or 1:5m transporter:lipids ratio, respectively) or were added to the vesicle suspension and thermostated at 25°C for 2 min. If protonophore CCCP was used, it was added to the liposomes as a solution in methanol (5 μL of 60 μM solution, to create a 1:1k protonophore:lipids ratio) and thermostated at 25°C for 2 min. prior to addition of base.

Fluorescence emission at 511 nm was recorded as a function of time over 5 min. for two different excitation wavelengths, 403 and 455 nm. Buffered aqueous solution of NMDG (30 μL, 0.5 M in 100 mM NMDGHCl + 10 mM HEPES) was added to the vesicle suspension 30 s after the start of the emission recording, to create a pH gradient of 1 unit (6.8 inside vs. 7.8 outside). Detergent (50 μL, Triton X-100, 5% w/w in water) was added 200 s after addition of bicarbonate to lyse liposomes. Fluorescence data were collected for at least two runs. The fluorescence ratios (excitation at 455 nm/403 nm) were calculated and the resulting data were normalised from 0 (before the addition of base pulse) to 1 (after lysis).

4.2 $H^+(OH^-)/Cl^-$ transport by anionophores **1-4** in NMDGHCl (HPTS assay)

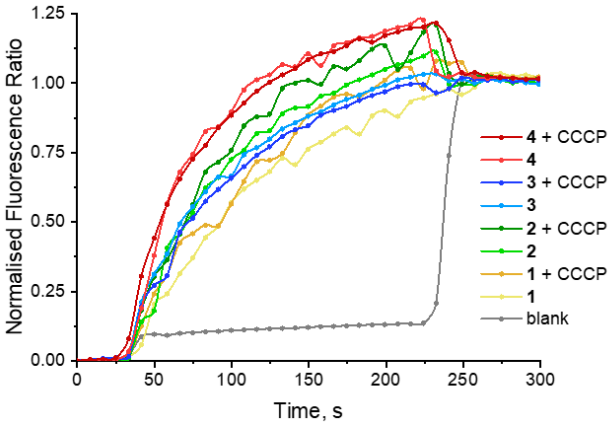

Figure S4.2. Normalised fluorescence ratio as a function of time in the HPTS assay for transporters **1**-**4** (1:100k) and combination of **1**-**4** (1:100k) + CCCP (1:1k). Medium: 100 mM NMGDHCl + 10 mM HEPES, pH 6.8. Transporters were added as DMSO solutions. At t = 30 s, 5 mM NMGD was added to increase the pH_{out} to 7.8. The LUVs were lysed 3 minutes after the base pulse. No differences in the presence of protonophore CCCP indicates that H^+ transport by **1**-**4** is not the rate-limiting process in this assay.

4.3 Calculations of EC_{50} values for $H^+(OH^-)/Cl^-$ transport by **1-4**

Hill analysis was performed using Origin 2022 software, by plotting normalised fluorescence intensity at t = 200 s against the transporter concentration in mol%.

The following equation (Hill1) was fitted to the experimental data:

$$y = START + (END - START) \cdot \frac{x^n}{(k^n + x^n)}$$

where k is the EC_{50} concentration at 200 s, and n is the Hill coefficient.

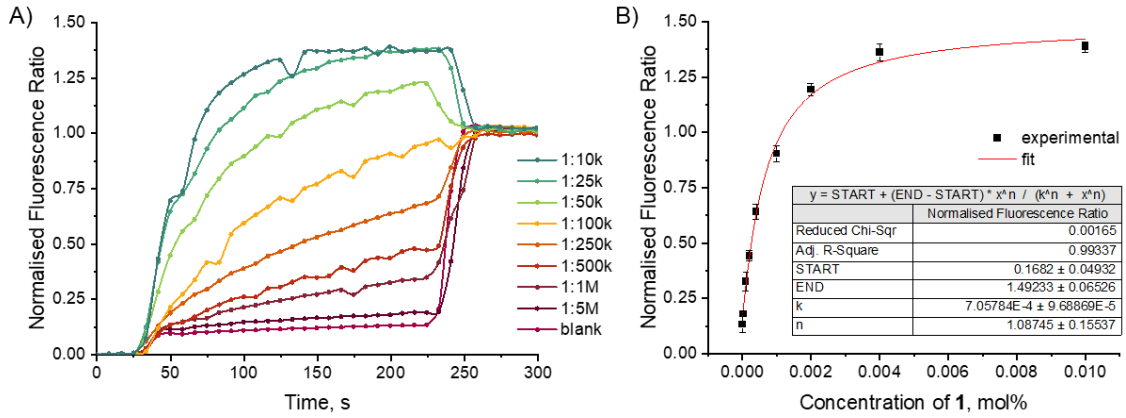

Figure S4.3.1. A) Kinetic traces from HPTS assay for compound **1** at varying concentrations (POPC:cholesterol 7:3 liposomes loaded with 1 mM HPTS, suspended in 100 mM NMDGHCl + 10 mM HEPES). B) Hill plot for compound **1**, including fitted curve and calculated $EC_{50,\ 200s}$ value.

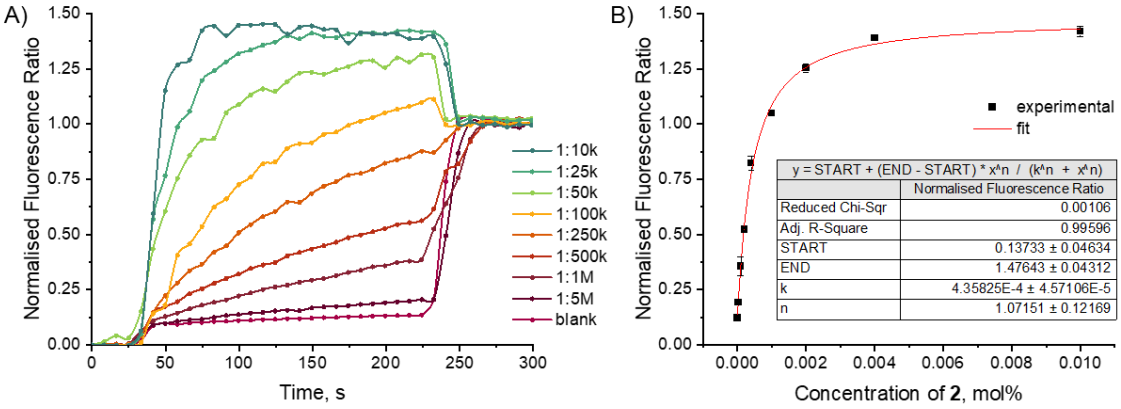

Figure S4.3.2. A) Kinetic traces from HPTS assay for compound **2** at varying concentrations (POPC:cholesterol 7:3 liposomes loaded with 1 mM HPTS, suspended in 100 mM NMDGHCl + 10 mM HEPES). B) Hill plot for compound **2**, including fitted curve and calculated $EC_{50,\,200s}$ value.

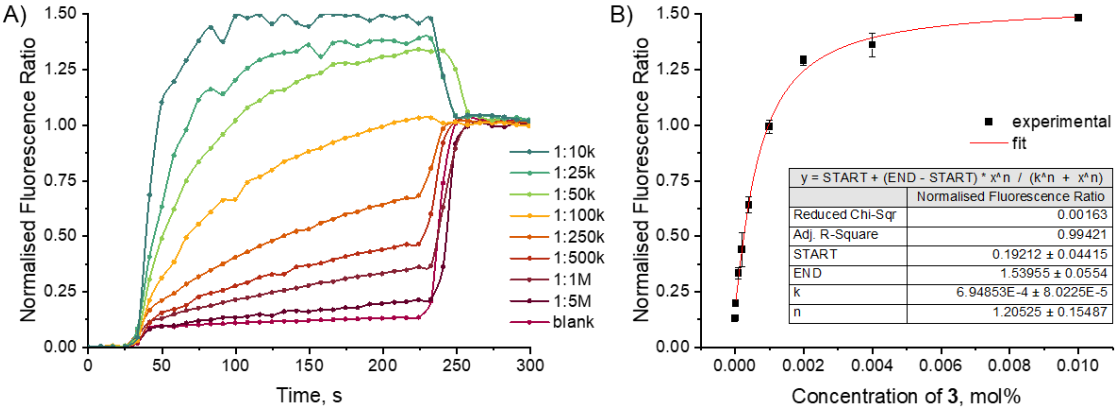

Figure S4.3.3. A) Kinetic traces from HPTS assay for compound **3** at varying concentrations (POPC:cholesterol 7:3 liposomes loaded with 1 mM HPTS, suspended in 100 mM NMDGHCl + 10 mM HEPES). B) Hill plot for compound **3**, including fitted curve and calculated $EC_{50,\,200s}$ value.

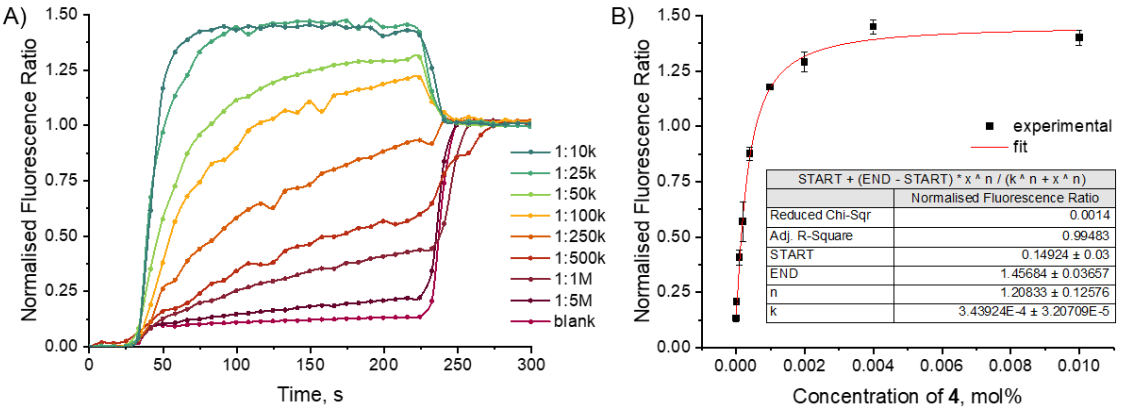

Figure S4.3.4. A) Kinetic traces from HPTS assay for compound **4** at varying concentrations (POPC:cholesterol 7:3 liposomes loaded with 1 mM HPTS, suspended in 100 mM NMDGHCl + 10 mM HEPES). B) Hill plot for compound **4**, including fitted curve and calculated $EC_{50,\,200s}$ value.

5 Biological studies

Bacteria strains used in this study: *Bacillus subtilis* (ATCC 168), *Staphylococcus aureus* (ATCC 25923), *Escherichia coli* (ATCC 25922), *Acinetobacter baumannii* (ATCC 17978).

5.1 General procedure for MIC and IC_{50} determination

All bacteria strains were obtained from ATCC and grown on a solid-state lysogeny broth (LB) medium. For all experiments, single bacteria colonies were suspended in fresh LB medium to obtain an optical density OD_{600} = 0.05. Assay was performed in 96-well culture plates. Each well was filled with 196 μL of bacterial culture and 4 μL of DMSO solution of compound **1**, **2**, **3** or **4** at different concentration (6 nM – 7.5 mM, obtained by serial 2-fold dilutions of a concentrated stock solution), pure DMSO or pure LB (for control experiments), so that the final volume in each well was 200 μL. The DMSO concentration was kept constant at 2% (v/v) in all experiments.

The cultures were grown at 30 °C (*B. subtilis*) or 37 °C (*E. coli*, *S. aureus*, *A. baumannii*) overnight. The OD_{600} was monitored spectroscopically after 24 h. Every experiment was performed in triplicate, using independent bacterial cultures. The minimum inhibitory concentrations (MICs) were determined as the concentration of receptor in which the bacteria growth is inhibited by ≥80%.

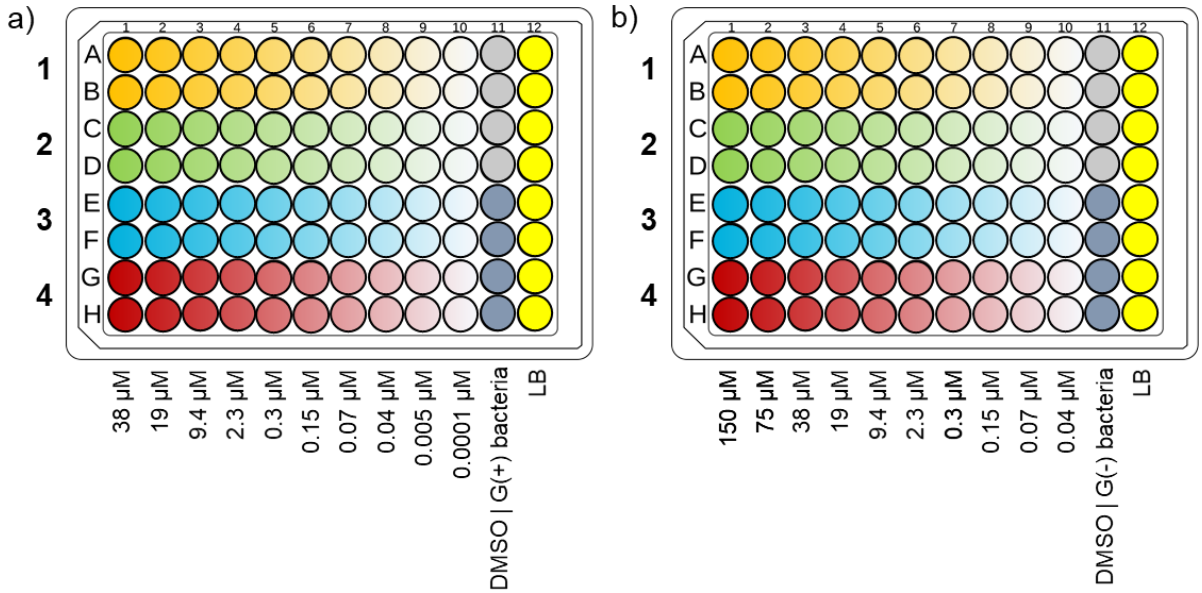

Figure S5.1. Scheme of examplary 96-well plate during the MIC determination experiment for transporters **1**-**4** at different concentrations. a) Gram-positive bacteria, b) Gram-negative bacteria. Dark-grey – control with LB + bacteria + 4 μL of DMSO; light-grey – control with LB + bacteria; yellow – control with pure LB.

5.2 Antibacterial properties of transporters **1-4** on Gram-positive bacteria

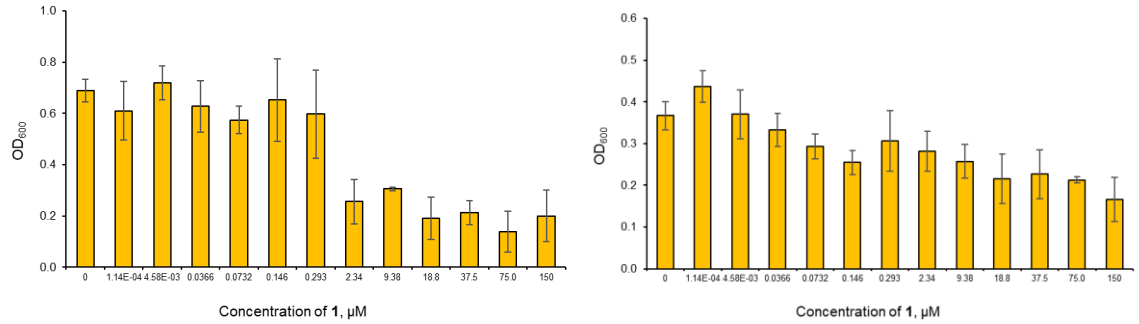

Figure S5.2.1. Plot of averaged optical density for Gram-positive *B. subtilis* (left) and *S. aureus* (right) in the presence of transporter **1** at different concentrations.

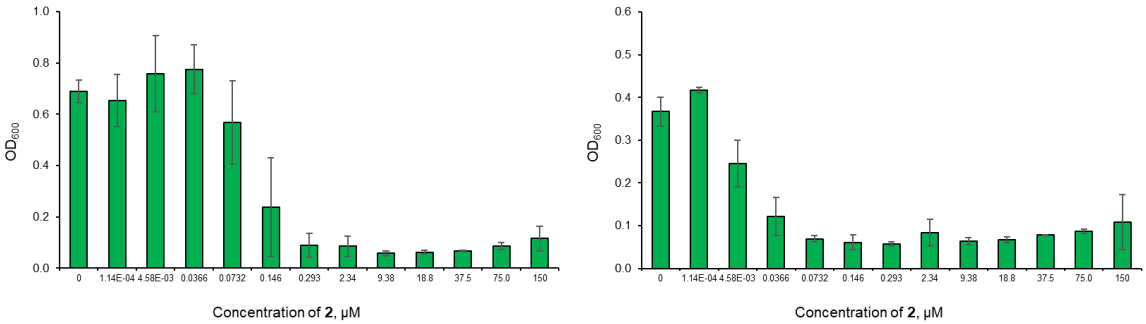

Figure S5.2.2. Plot of averaged optical density for Gram-positive *B. subtilis* (left) and *S. aureus* (right) in the presence of transporter **2** at different concentrations.

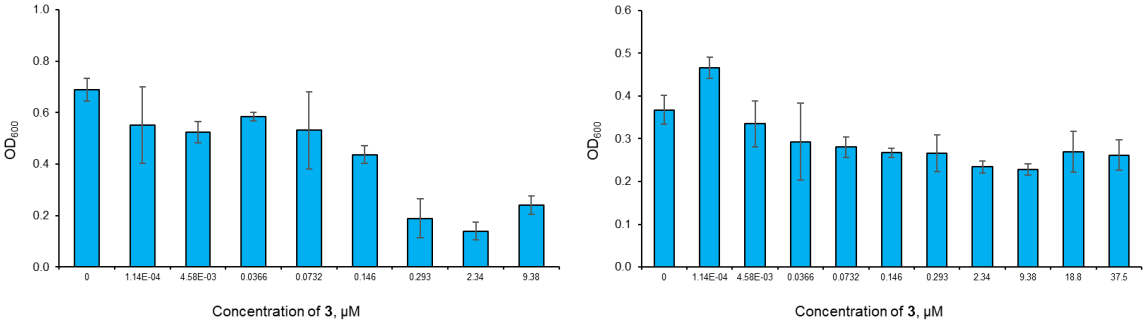

Figure S5.2.3. Plot of averaged optical density for Gram-positive *B. subtilis* (left) and *S. aureus* (right) in the presence of transporter **3** at different concentrations.

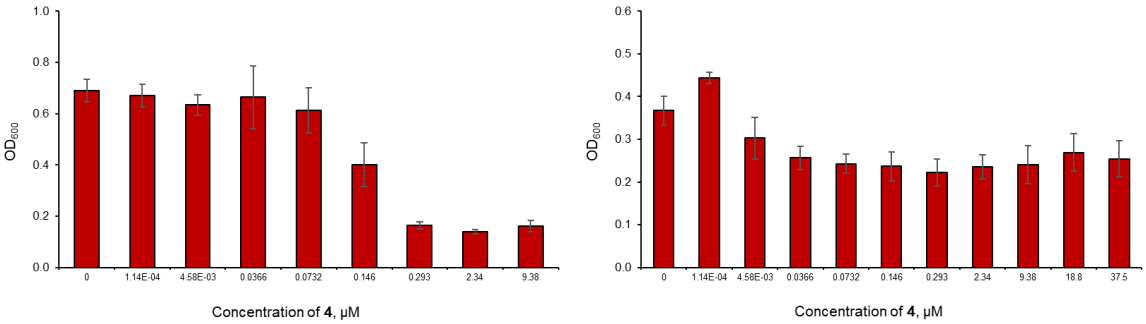

Figure S5.2. Plot of averaged optical density for Gram-positive *B. subtilis* (left) and *S. aureus* (right) in the presence of transporter **4** at different concentrations.

5.3 Antibacterial properties of transporters **1-4** on Gram-negative bacteria

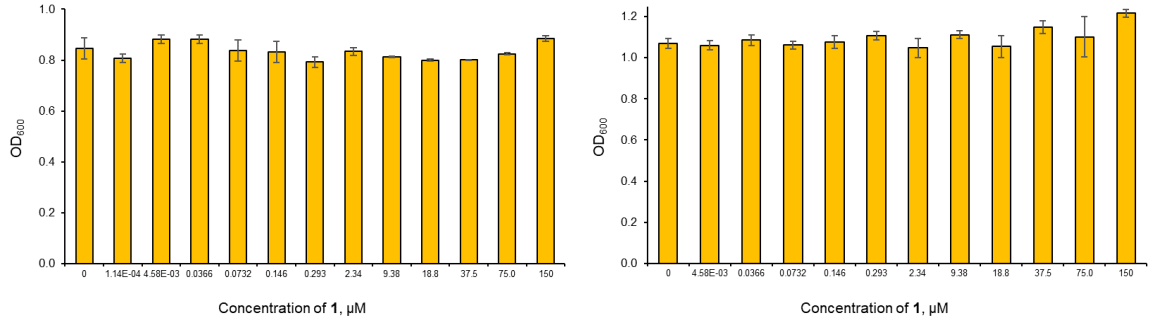

Figure S5.3.1. Plot of averaged optical density for Gram-negative *E. coli* (left) and *A. baumannii* (right) in the presence of transporter **1** at different concentrations.

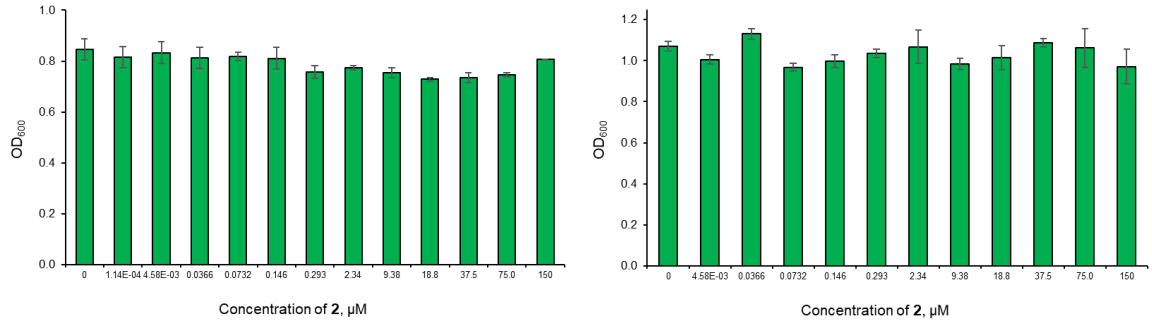

Figure S5.3.2. Plot of averaged optical density for Gram-negative *E. coli* (left) and *A. baumannii* (right) in the presence of transporter **2** at different concentrations.

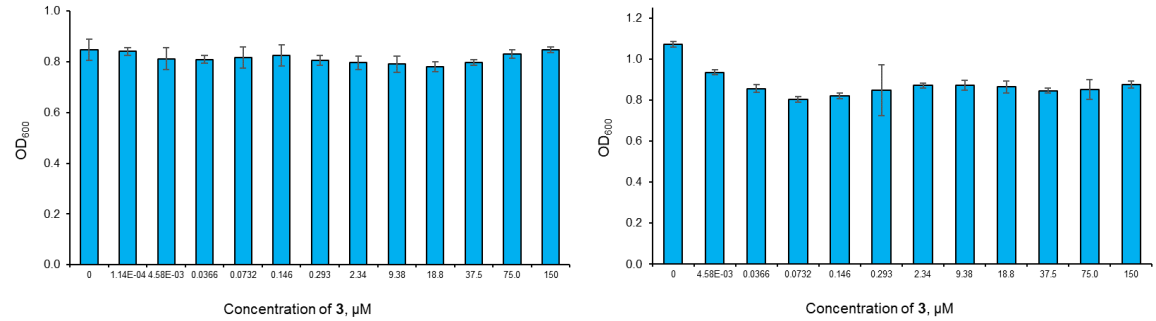

Figure S5.3.3. Plot of averaged optical density for Gram-negative *E. coli* (left) and *A. baumannii* (right) in the presence of transporter **3** at different concentrations.

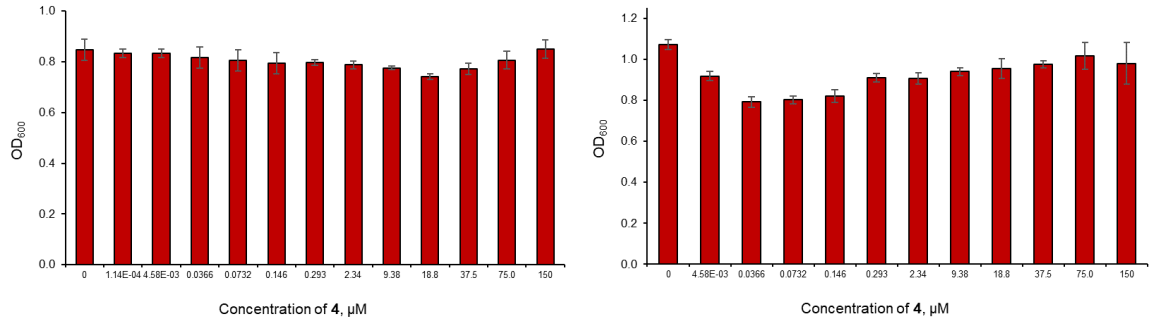

Figure S5.3.4. Plot of averaged optical density for Gram-negative *E. coli* (left) and *A. baumannii* (right) in the presence of transporter **4** at different concentrations.